A Multikilowatt X-Band Nanosecond Source

HARRY GOLDIE, MEMBER, IEEE

Abstract—**A new technique is presented which furnishes an exceptionally narrow pulse of 6 to 12 ns duration with steep skirts of 1 to 3 ns at peak power levels of tens of kilowatts. The pulse is derived by means of two sequential discharges in a nonresonant waveguide section. An analysis of the low-pressure breakdown of a gas under the action of intense microwave fields considerably higher than the threshold of breakdown field shows that under certain optimum combinations of gas parameters the aforementioned pulse is obtained.**

Experimental results show that a 70 kW rectangular pulse of 12 ns width with 2 ns skirts can be reliably generated on a repetitive basis with negligible jitter.

Background

HISTORICALLY, the motivation for detailed studies of low-pressure microwave gas breakdown has always arisen from either the need to attain a better understanding of the spike leakage phenomenon characteristic of T–R cavities[1] or to find the maximum power limitations of satellite-borne antennas which are immersed in a low-pressure environment.[2],[3] Work to enhance the high-power capabilities of a triggered waveguide switch[4] employing a low-pressure gas has been recently investigated. The reduction in RF breakdown power of high-Q T–R devices is a fundamental operating requirement, and most investigations in that area are directed toward reduction of spike leakage energy. The investigations of antennas immersed in low-pressure gases, notably air, are useful for determining the maximum radiating power limitations due to breakdown as a function of altitude. With regard to the triggered waveguide switch there are no resonant structures; and one attempts to enhance the RF breakdown power by varying the geometry and the nature and pressure of the gas. These are the essential parameters since they determine the peak power switching capacity of this class of device.

The phenomenon which is reported in this paper concerns the development of a high-power narrow rectangular pulse which is derived from a longer pulse. This is accomplished by sequential breakdown in two sections of a transmission line, each of which contains a low-pressure gas acted upon by relatively intense applied fields. Consequently, we will be concerned with the buildup of microwave attenuation to relatively high values within time periods approaching several nanoseconds. The problem of implementing such techniques, aside from its fundamental aspects, is of interest from the viewpoint of its engineering applications, particularly in radar systems. Developing a source to generate relatively high-power pulses of nanosecond duration provides a radar with extremely high target resolution.

It will be shown that the techniques described herein can be used to generate multikilowatt microwave pulses of nanosecond duration; moreover, by adjustment of trigger delays applied to the two low-pressure discharges, a high-power pulse of variable width from tens of nanoseconds to the full width of the input pulse can be obtained. This latter method differs from the extremely narrow pulse technique in that the microwave power itself does not initiate the gas breakdown.

Manuscript received May 17, 1967.

The author is with the Microwave Technology Laboratory, Westinghouse Defense and Space Center, Baltimore, Md.

Introduction

The leading edge of a microwave high-power pulse, when viewed on a nanosecond scale, regardless of the type of tube used as the source, appears as a ramp function whose power level rises from zero to a maximum value equal to the peak amplitude characterized by the flat portion of the pulse. If this same pulse is incident on a waveguide section containing a low-pressure gas which is enclosed by a pair of windows acting only as pressure barriers, and if the intensity is sufficiently high, a breakdown of the gas will result. Assuming the insertion loss of the short section of line containing the gas to be negligible then the incident and transmitted power will rise identically until the gas breaks down initiating a discharge. If the microwave conductivity of the ensuing discharge is sufficiently high, the transmitted pulse will rapidly fall toward zero.

Under conditions of high electron density and low collision frequency, relative to the applied signal frequency, the conductivity will be large; and the discharge acts as an effective barrier to the remainder of the incident pulse. The rising portion of the reflected pulse as well as the falling edge of the transmitted pulse will be controlled by the time required for the electron density to rise from a value corresponding to negligible RF attenuation to a value of electron density corresponding to a relatively high degree of attenuation. This situation is illustrated in Fig. 1. By creating experimental conditions which increase T_1 to where it encompasses the total ramp interval of the incident pulse, and which simultaneously decrease T_2 to values of only a fraction of T_1, then the rising portion of the reflected wave (up to the maximum source amplitude) will occur at a rate far exceeding the original rate of rise of the incident pulse.

The breakdown of a gas under the action of intense fields is defined as the transition of the electron density in the gas from some relatively low initial value to a density orders of magnitude greater at which a steady-state condition exists. The threshold of breakdown is taken as that value of applied field at which the production and loss rate of elec-

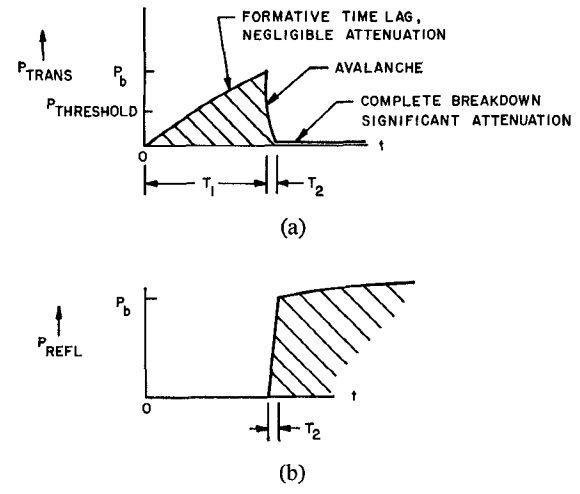

Fig. 1. Formation of leading edge in first discharge. (a) Transmitted pulse. (b) Reflected pulse from discharge.

trons are equal ($P_e - L_e = 0$). A slight increase of the field beyond this value will cause the electron density to increase several orders of magnitude to where a dynamic equilibrium will exist between the production and loss rate of electrons; this avalanche results in complete breakdown.

The rate of increase in electron density is slow during the interval T_1 relative to the increase in electron density during the interval T_2. These intervals correspond to the period leading to the avalanche and the avalanche period itself. Their duration is experimentally determined by the associated values of RF attenuation as shown in Fig. 1. Here T_1 is the time lag from the initiation of the ramp pulse to where attenuation of this same pulse becomes significant ($\sim$0.3 dB); T_2 is the time lag corresponding to the avalanche which initiates at a very low value of attenuation ($\sim$0.3 dB) and continues to where the attenuation of the transmitted pulse is significant ($>$10 dB)

Both T_1 and T_2 are functions of the rate of rise and magnitude of the applied field, nature and pressure of the gas, initial density, and geometry. The conditions which simultaneously produce a maximum T_1 and a minimum T_2 are of interest. Therefore, analysis is directed toward an optimum selection of combinations of these parameters in order to yield information for the efficient derivation of an extremely short pulse of rectangular characteristics whose peak amplitude approaches that of the longer source pulse.

The experiments performed were limited to hydrogen gas at pressures of 0.12 to 0.37 torr contained in WR 112 copper waveguide and acted upon by midplane waveguide fields of 3.6 to 7.2 kV/cm (50 to 200 kW) propagating in the TE_{10} mode at a frequency of approximately 9400 MHz. The range of applied fields used exceeded the threshold-of-breakdown field for the above range of pressures. Hydrogen was selected because of its relatively low collision probability at high electron energies, also because of extensive breakdown work previously done on this gas thus giving readily accessible experimental coefficients, and for the reason that the pressure can be simply controlled by a commercially available hydrogen replenisher.

Remanent Electron Density

Experimental investigations of microwave breakdown of a low-pressure gas require an initial electron density to be present in the discharge space prior to breakdown. This prevents statistical fluctuations in breakdown energy which would occur if the natural background density was not sufficiently masked. Normally, this initial density is provided either by an appropriately located dc discharge or by a radioactive source embedded in the discharge space. These priming sources create a relatively low density ($\sim 10^7$ to 10^8 electrons/cm^3) whose spatial distribution is both nonuniform and highly localized relative to the field distribution in the waveguide.

Assuming the pressure, applied field, and geometry are constant, then the formative time T_1 is a function of the spatial distribution of electrons, their distribution of velocities, and their initial number density over the volume of the waveguide where the applied field is relatively high. By creating experimental conditions such that the applied field sees: a) an initial density sufficiently high to mask the background density, b) a uniform distribution of electrons in the center half of the waveguide, and c) a Maxwellian distribution of electron speeds with an average temperature of a fraction of an electronvolt (isothermal inactive plasma), one provides optimum conditions to obtain a jitter-free breakdown interval with a reproducible breakdown characteristic when operation is repetitive at a high PRF. Ideally, each differential cross-sectional element of the applied field over the center half of the waveguide should see a gas surface where each infinitesimal element contains equal number densities and identical velocity distributions. Thus, the charge densities build up uniformly over the discharge region as in a bulk interaction; the consequence is a stable and reproducible breakdown with each succeeding pulse. With radioactive or dc priming sources, the action of the field is to increase the charge density first in the local region where the initial density is high and then to depend upon diffusion gradients to initiate a volume breakdown. These diffusion gradients require a finite time to spread the electrons throughout the volume, the interval being a function of the initial distribution and instabilities in the priming sources. Therefore, the charge gradients may fluctuate with each successive breakdown, the result being a jitter in breakdown amplitude and in T_1.

The desired charge distribution discussed which has been defined as the remanent density is approximated by forming a sheet beam of electrons in the section of the transmission line illustrated in Fig. 2. The beam creates a plasma of approximately 10^{11} to 10^{12} electrons/cm^3 which is then allowed to decay. In the early afterglow the density, rate of diffusion, and temperature of the electrons are high. Late in the afterglow, however, the electrons lose all trace of their ordered motion and rapidly thermalize approaching an isothermal plasma; the electrons then decay by a combination of ambipolar and free diffusion.

We can approximate the time required for the electrons to lose their energy relative to the charge density

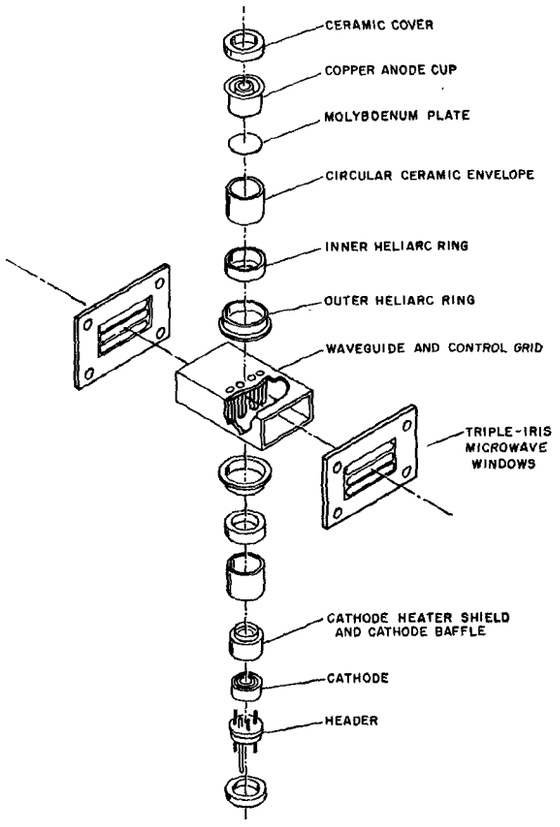

Fig. 2. Exploded view of low-pressure section of the line.

decay τ_d by considering the time constant τ_e for elastic collisions only. This will give the upper limit of τ_e because if the effects of inelastic collisions were included the electrons would cool more rapidly. Thus, $\tau_e=(G\nu_c)^{-1}$ where the fractional loss in energy for hydrogen is $G=2m/M=5.3\times10^{-4}$ and the collision frequency $\nu_c=5.93\times10^9\ p_0$ is independent of electron energy; here p_0 is taken as 0.2 torr. The result yields $\tau_e=1.57$ μs. Low-pressure hydrogen plasmas decay only by diffusion, and the densities being considered are sufficiently high so that the diffusion is primarily ambipolar. The time constant characterizing charge decay is $\tau_d=\Lambda^2/D_a$, where the characteristic diffusion length for the WR 112 waveguide is $\Lambda=0.355$ and the ambipolar diffusion coefficient-pressure product is $D_ap_0=700$ cm^2/s/torr. Inserting these values yields $\tau_d=36$ μs, and taking the ratio τ_d/τ_e indicates that the electron temperature decays orders of magnitude before the number density decays to 37 percent of its maximum value. Thus, for our experimental conditions the electrons cool much more rapidly than the density decays, and an isothermal plasma in the late afterglow is obtained.

The source pulse applied to break down the gas is delayed so that it is incident on the low-pressure waveguide section during the late afterglow when the conditions discussed prevail. The time delay between the initiation of the beam to produce the remanent density and the arrival of the source pulse is not critical because the remanent density late in the afterglow period is changing relatively slowly compared to the risetime of the high-power source pulse.

Therefore, it may be concluded that the remanent density provides an inactive plasma suitable to facilitate repeatable breakdown characteristics with each applied pulse; in effect we have created favorable conditions for reflected power leading edge pulse stability. Interpreted in terms of a repetitive output pulse, the peak output power will remain constant, the rate of rise of the reflected pulse will repeat identically, and the location in time of the initiation of breakdown (analogous to leading edge jitter) will not fluctuate.

Microwave Breakdown

The energy required for breakdown under the action of an applied RF field can be made independent of external influences as discussed above. However, the high remanent density tends to decrease the breakdown level limiting the power of the output pulse. To estimate the magnitude of this dependence the general breakdown relation is stated as

$$\frac{\partial n}{\partial t} = P_e - L_e \tag{1}$$

where $P_e=\nu_i n+R$ is the production rate of electrons, ν_i is the ionization rate, and R is the production rate due to secondary sources, such as the remanent density, and L_e is the electron loss rate. Threshold of breakdown occurs when $\partial n/\partial t=0$ and is experimentally determined by slowly increasing the RF power of a CW source until equilibrium is established. A solution of (1) for the pulsed case, where diffusion-controlled breakdown dominates, yields[5]

$$\frac{1}{T_p}\ln\frac{n_b}{n_r} = \nu_i - \frac{D}{\Lambda^2} \tag{2}$$

where

$\nu_i/p_0=f(E_e/p_0)$ and is determined by experiment
n_b = the critical density required to initiate the avalanche
T_p = the width of the applied pulse
D = either the free or ambipolar diffusion coefficient or a combination of both, depending on the charge density.

It becomes evident that n_r, being a logarithmic function, has a small effect on the breakdown level; a density ratio change of 100 affects the left-hand term by a factor of 2.

Any significant losses occurring during T_1 or T_2 must be compensated for by the applied field. Since ambipolar diffusion is a relatively slow process, the only loss to be considered during T_1 would be free diffusion. An estimate of this loss magnitude can be made by computing the time t_d it takes for an electron to diffuse to the wall from the center of the waveguide. Thus

$$t_d = \frac{3\Lambda^2}{2l^2\nu_c} = 12.8\times10^{-9}p_0 \qquad \text{(seconds)}$$

where $l=(p_0P_c)^{-1}$ is the electron mean free path. The probability of a collision at electron energies above several electronvolts is $P_c=20$ cm^2/cm^3. A pressure of 0.2 torr yields a diffusion time $t_d=2.6$ ns which is considerably shorter than the interval T_1 but is comparable to T_2. It may

be concluded that large electron losses can occur during T_1 relative to T_2 which must be compensated for by an increase in the applied field; the consequence is a slight increase in breakdown power.

The dominant energy loss mechanism during T_2 is elastic and inelastic collisions in the body of the gas and not diffusion to the walls. The intervals differ markedly in that losses during T_1 are affected primarily by geometry, while T_2 losses are affected by the total collision frequency. Regardless of the loss mechanism, the applied field must compensate for the energy losses if the net ionization is to increase the charge density. In both intervals the power applied to break down the gas is a function of the energy losses; the rate of power dissipation in the gas during T_2 being much larger than during T_1.

The applied field does not raise the energy of the electron instantaneously. A lag between the energy accumulated by the electron gas and the applied field is relevant since it increases T_1. The magnitude of this effect can be found by assuming an applied stepfield as follows:[6]

$$\Delta t = \frac{\Delta u m(\omega^2 + \nu_c^2)}{e^2 E^2_{\text{rms}} \nu_c} \qquad \text{(seconds)}$$

where Δu is the change in average energy of an electron, E_{rms} is the midplane waveguide field, and Δt is the delay suffered by an electron in following the field. Computations for a field of 3.6 kV/cm and $\Delta u = 15.4$ eV (ionization potential of molecular hydrogen) at pressures of 0.2 torr yield $\Delta t = 2$ ns. We may conclude that the electron energy time lag is negligible compared to interval T_1 and it will be neglected in subsequent discussions.

Optimizing T_1

To realize the full potential of this technique the breakdown interval T_1 must be equal to or greater than the rise-time of the source pulse. This situation is qualitatively depicted in Fig. 3 where the breakdown power as a function of rate of rise of source power is shown. The dashed curve illustrates the criterion for maximum efficiency and optimum utilization of the source. For constant remanent density pressure and geometry, the interval T_1 is a function of the rate of rise of the applied field. We have previously shown that under special conditions the remanent density would result in a breakdown characteristic having a minimum of jitter and a maximum of reproducibility.

One of the most important variables in gas discharges is pressure; its effect will be discussed with regard to optimizing T_1. In the presence of collisions Newton's second law is

$$m\frac{dv}{dt} + m\nu_c v = -eE_0 \exp(j\omega t).$$

The rate of gain of energy of the electrons is $P = eE_{\text{rms}}v$ and the solution for power gain yields[7]

$$P = \frac{ne^2E^2_{\text{rms}}}{m\nu_c}\left(\frac{\nu_c^2}{\omega^2 + \nu_c^2}\right) = \frac{ne^2E_e^2}{m\nu_c}.$$

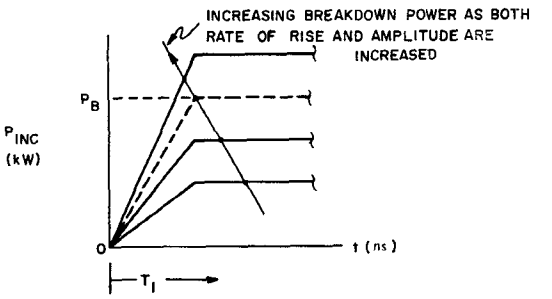

Fig. 3. Breakdown power as a function of source power.

This result shows that the transfer of energy to the gas is inefficient at low pressures ($\nu_c \ll \omega$) where the fields make many oscillations per electron-molecule collison. This inefficient transfer of RF power to the gas is extremely useful in delaying the charge buildup (increasing the formative time lag) and, hence, extending T_1. Maximum energy transfer efficiency occurs when $\nu_c = \omega$, a pressure of 10 torr for H_2, which is far above the experimental pressure of 0.2 torr. E_e is the field effective on the discharge and is equivalent to a dc field producing the same energy transfer. The average energy the electrons accumulate is a function of E_e/p_0 where

$$E_e = E_{\text{rms}}[1 + (\omega/\nu_c)^2]^{-1/2}$$

where E_{rms} is the applied field in the waveguide midplane. We can compute ω/ν_c for a pressure of 0.2 torr at 9400 MHz to obtain

$$\frac{\omega}{\nu_c} = \frac{2\pi(9.4 \times 10^9)}{5.93 \times 10^9 p_0} = \frac{10}{p_0} = 50.$$

Thus, $E_e \approx 0.02\ E_{\text{rms}}$ which represents an energy transfer efficiency of 2 percent. The fields corresponding to 50 and 200 kW are 3.6 and 7.2 kV/cm; however, the fields effective on the discharge E_e are 72 and 144 V/cm corresponding to E_e/p_0 values of 360 and 720 V/cm/torr, respectively. It is this poor efficiency which allows the source field incident on the first discharge to rise to high values encompassing a large fraction of the interval T_1 before breakdown occurs.

We are actually causing two competing processes; the high remanent density tends to decrease the breakdown level, and the lower pressures tend to increase the breakdown power. The latter process is made dominant; however, the limit to which the pressure can be decreased is restricted by the dimensions of the container and the maximum ordered amplitude of the electron gas. Too low a pressure under intense fields will cause the electrons to be swept to the waveguide wall as in a dc discharge. If secondary emission processes at the walls were negligible, the field required for breakdown would rapidly rise. However, if the wall is a good source of secondary emission, then the walls, not the gas, would play a prominent part in the discharge. This is undesirable from the viewpoint of stability and jitter since the secondary emission coefficient varies with the history of the surface and is not constant with time.

The pressure limitation may be calculated if half the distance L between the broadwalls of the waveguide is set as a criterion for the maximum mean free path l. We find

$$p_0 \geq \frac{1}{\left(\frac{L}{2}\right)P_c} \qquad \text{(torr)}$$

where the probability of a collision P_c is determined from experimental results.[7] Inserting $L/2=0.6$ cm and $P_c=20$ it is found that $p_0 \geq 84$ mtorr.

The limiting case for the maximum amplitude of ordered electron motion is determined by setting the peak displacement $X_p=L/2$ as follows:

$$X_p = \frac{2eE_{\text{rms}}}{m\omega(\omega^2+\nu_c^2)^{1/2}} = 0.6$$

which yields 860 kV/cm. This is far in excess of the fields to be used, and it must be concluded that ordered motion will not cause a sweeping of the electrons to the wall regardless of pressure. For a field of 7.2 kV/cm the ordered displacement is 0.052 mm; which is considerably smaller than the 6 mm half-height of the waveguide.

It may be concluded that T_1 can be increased by lowering the pressure beyond the point where the efficiency of energy transfer becomes low enough to overcome the effects of a high remanent density. The lowest operating pressure is limited to where $l=L/2$; a decrease in pressure below this point yields a wall-dependent breakdown value which is too unstable for a practical repetitive pulse system.

Reflected Power

During T_2 the avalanche builds up rapidly and the applied field is attenuated. Within the plasma the field is both increased and decreased simultaneously. It is increased because the wave is traversing a medium of negative permittivity and decreased as a result of power losses in the discharge and a change in wavelength. This latter effect results in a waveguide below cutoff and for our experimental conditions dominates, whereas the former two effects can be treated as perturbations. At the conclusion of T_2 the plasma reaches a state of dynamic equilibrium in which the charge density approaches values $\geq 10^{11}$ electrons/cm^3 and the ratio f_p/f, where f_p is the plasma resonance frequency and equals 8970 $\sqrt{n}$, exceeds unity.

Whether the plasma becomes a good reflector or absorber of microwaves, however, depends on ν_c/ω. An examination of the relation for the reflection coefficient[8]

$$\frac{\text{reflected power}}{\text{incident power}} = \left| \frac{(1-\epsilon_c)[1-\exp(4\pi j\sqrt{\epsilon_c}d/\lambda)]}{(1+\sqrt{\epsilon_c})^2-(1-\sqrt{\epsilon_c})^2\exp(4\pi j\sqrt{\epsilon_c}d/\lambda)} \right|^2$$

for an established plasma in a transmission line assumed to have a uniform electron distribution reveals that when $\nu_c \ll \omega$ and $\omega_p > \omega$, as in the case under discussion, a major fraction of the incident power is reflected. This relation is plotted in Fig. 4 for $f_p/f \geq 1$ and an electrical length of $d/\lambda = 0.75$. The small fraction of power which is absorbed is due to collisions and electron losses. In a plasma assumed to be in dynamic equilibrium with the applied field this is referred to as arc loss. The complex plasma dielectric constant is $\epsilon_c = 1+\omega_p^2/[j\omega(\nu_c+j\omega)]$.

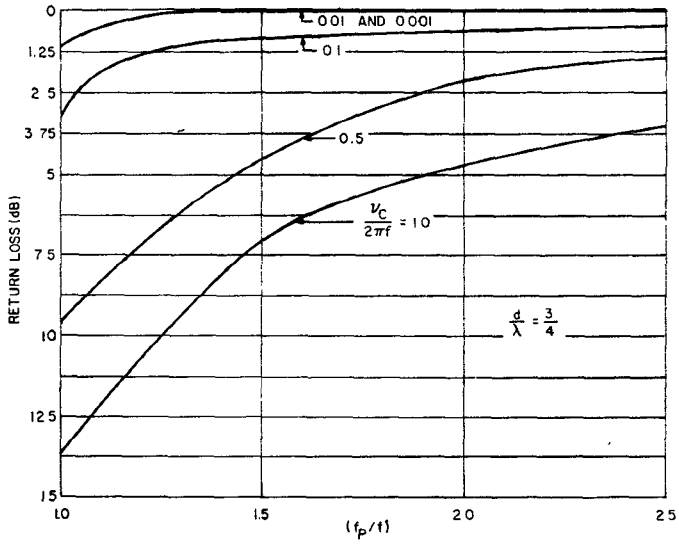

Fig. 4. Return loss from a plasma of uniform density as a function of f_p/f with ν_c/ω as a parameter.

We may conclude that the maximum amplitude of the reflected power does not reach the peak value of the source pulse when $\nu_c < \omega$ and that this is a limitation of this technique. However, under the experimental conditions of $\nu_c \ll \omega$, the reflected power can be made to closely approach the incident power level as shown in Fig. 4.

Optimizing T_2

T_2, the time for the transmitted pulse to attenuate from 0.3 to >10 dB, is characterized by an avalanche buildup in electron density from n_b to n_p where n_p is the electron density when the plasma reaches dynamic equilibrium. This buildup spans orders of magnitude of electron density and the dominant electron loss mechanism of the active plasma changes from diffusion to collisional losses. The primary energy loss mechanism during T_2 is due to inelastic collisions; moreover, the electron energy is high under the action of intense fields (~10 to 15 eV); therefore; the average rate of energy loss is high. It is this high rate of energy loss during T_2 which causes the rate of rise of reflected power to be smaller than the rate of fall of the transmitted power.

To obtain an interval T_2 relatively short compared to T_1, the buildup in charge density must occur in a few nanoseconds. It has been noted that the field increases during T_2 due to the onset of negative permittivity and it can be shown that the magnitude increases with decreasing pressure at a constant applied frequency.[1] However, the energy transferred to the electron gas is a maximum when $\nu_c=\omega$. Apparently T_2 will be a minimum at some pressure less than that at which $\nu_c=\omega$. This minimum occurs at a pressure where the efficiency of energy transfer from the field to the electrons becomes low enough to overcome the effect of the field enhancement due to the high density.

To compute the duration of this minimum at the optimum pressure requires a knowledge of how the field, ionization frequency, and electron density are changing during T_2. This is difficult and we have not done this. Nevertheless, the conditions for minimizing T_2 are compatible with increasing T_1, that is, by decreasing pressures below the value at which $\nu_c=\omega$. Note that the conditions for minimizing the jitter of T_1 are also compatible with buffering T_2 from the background density.

Formation of the Output Pulse

Having formed the steep wavefront by action of the first discharge, a second discharge occurring a brief interval later is used to form the lagging edge. The time lag T_1' to initiate the second discharge becomes the output pulsewidth and the avalanche interval T_2' becomes the lagging edge of the pulse. These time intervals are illustrated in Fig. 5; the circuitry used to derive the output pulse is shown in Fig. 6. A pulsetime diagram describing the operation of this circuit, assuming lossless components, is depicted in Fig. 7.

The time required to raise n_r to n_b in the second discharge is longer than the risetime of the applied field ($T_2<T_1'$) and, therefore, a stepfield incident on this second discharge is assumed. Under the same experimental conditions in both low-pressure wavegude sections, it would be expected that the interval $T_1>T_1'$ since the field incident on the second discharge is at its maximum value within 1 to 3 ns.

In the case of the second discharge, we wish to facilitate breakdown in order that the output pulsewidth be very narrow. This can be accomplished by increasing the pressure above that of the first discharge or, as an alternative, raising the remanent density to higher values. Upon breakdown, when T_1' ends and T_2' begins, the transmitted pulse begins to fall rapidly. The avalanche interval (defined as the time T_2' for the attenuation to rise from 0.3 to 10 dB) results in a high electron density effectively barring further propagation through the low-pressure section of line. The result is a rapid fall of the transmitted power thereby forming the lagging edge of the useful output pulse. Simultaneously, a reflected pulse with a steep wavefront is dissipated in a termination at port 4 as shown in Fig. 6.

The two discharges operate under similar experimental conditions. The small difference stems from the section of the useful output pulse which is formed by the particular discharge. The first discharge is critical since its breakdown determines the peak output power. Therfore, combinations of parameters which inhibit breakdown are used. The second discharge is not critical with respect to breakdown level since the wavefront is essentially a stepfield when compared with the formative time lag. Therefore, the pressure or remanent density may be set slightly higher in this second discharge, the primary effects of these two parameters being a variation in output pulse duration with negligible effect on the peak amplitude. Only at exceptionally high pressures in the second discharge in the range of $\nu_c=\omega$ will the amplitude of the useful output pulse be altered.

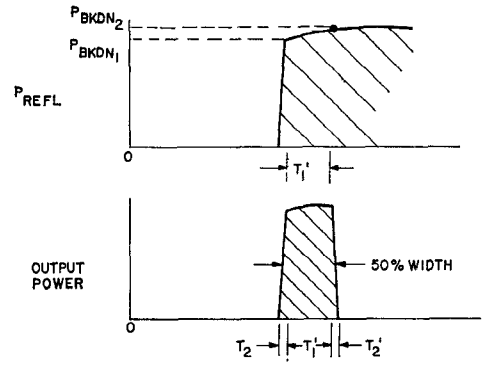

Fig. 5. Formation of lagging edge in second discharge.

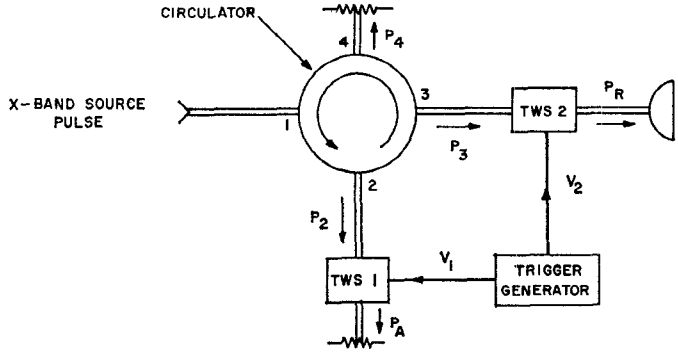

Fig. 6. Schematic of circuit.

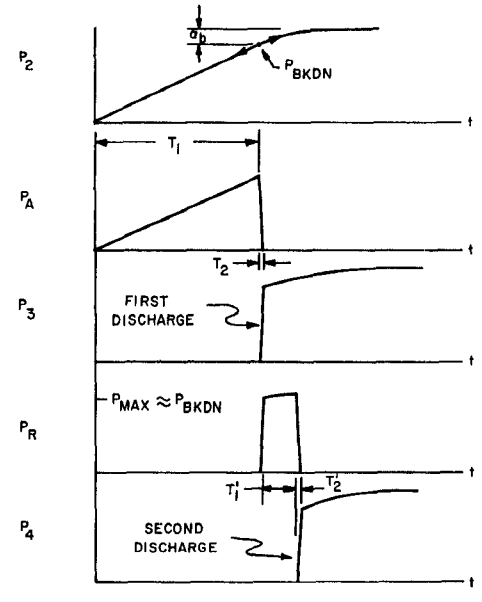

Fig. 7. Pulse-time diagram assuming lossless components.

X-Band Data

Experiments designed to yield high peak power rectangular pulses of nanosecond duration at 9400 MHz were performed. Two low-pressure sections of line (which will be referred to as TWS for triggered waveguide switches) containing hydrogen replenishers and heated cathodes were connected as shown in the circuit of Fig. 6. The cold loss and bandwidth of these devices are depicted in Fig. 8. The VSWR

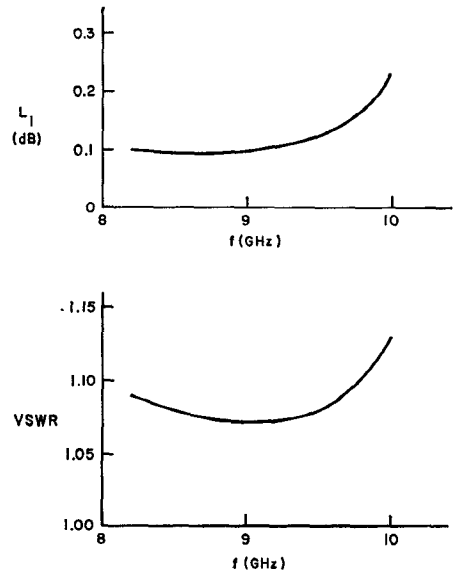

Fig. 8. Cold loss data. The curves are the average of four devices.

TABLE I

CIRCULATOR CHARACTERISTICS

Conditions	Ports	Measured Value
Matched conditions		
VSWR	1–1	1.29
Insertion loss	1–2	0.33 dB
Cross coupling	1–3	34 dB
Isolation	1–4	29 dB
With sliding short at port 2		
VSWR	1–1	1.25–1.30
Insertion loss	1–3	0.55–0.60 dB
Bandwidth for VSWR<1.4	1–1	1.77 GHz

is a result of the low-pressure windows used to form the vacuum envelope. The characteristics of the circulator are given in Table I. The port 1–3 measured loss with a metallic short replacing TWS No. 1 at port 2 and with TWS No. 2 at port 3 is 0.7 dB.

The pulse-time diagram including losses is shown in Fig. 9. The beam current used to excite the plasma and the resultant decaying electron density is also shown. The power limitation due to breakdown α_b when summed with the arc loss α_a of TWS No. 1 and the 0.7 dB cold loss determines the peak power of the output pulse.

T_1 and α_b as a function of hydrogen pressure with the remanent density as a parameter are presented in Figs. 10 and 11. The remanent density is given in terms of the delay between the cessation of the video excitation pulse and the point at which the RF field is applied to the TWS. The result shows both the breakdown field and T_1 decreasing with increasing pressure at constant remanent density. This is due to the steady increase in energy transferred from the applied field to the electron gas as a result of the decreasing mean free path. Fig. 12 shows the same data plotted as a function of remanent density (given as the delay time) for constant pressure. The breakdown power is a straight line

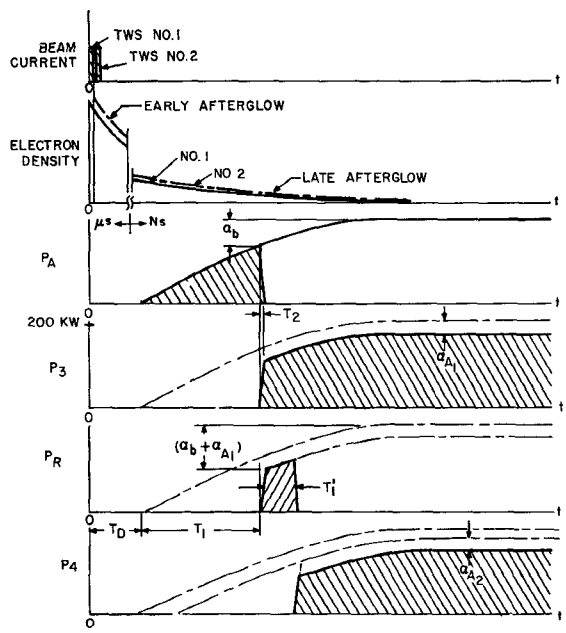

Fig. 9. Pulse-time diagram including component losses.

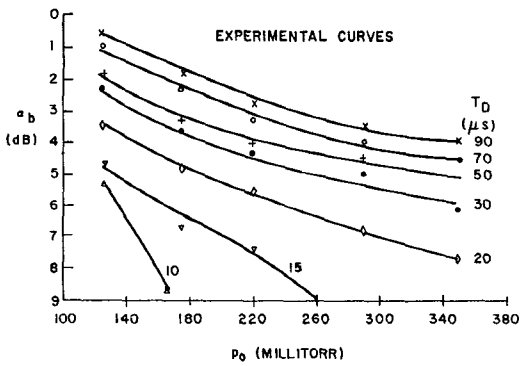

Fig. 10. Breakdown power as a function of pressure with remanent density as a parameter.

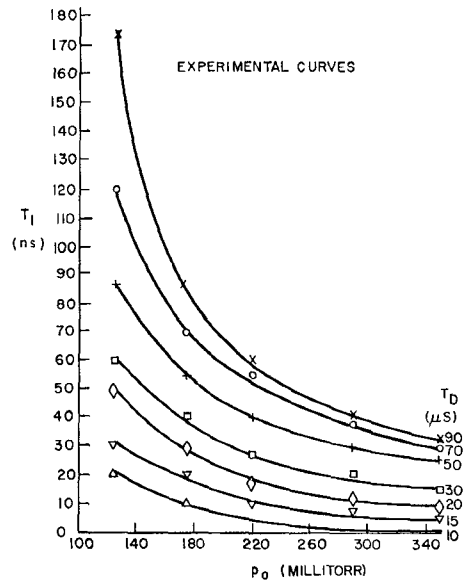

Fig. 11. T_1 as a function of pressure with remanent density as a parameter.

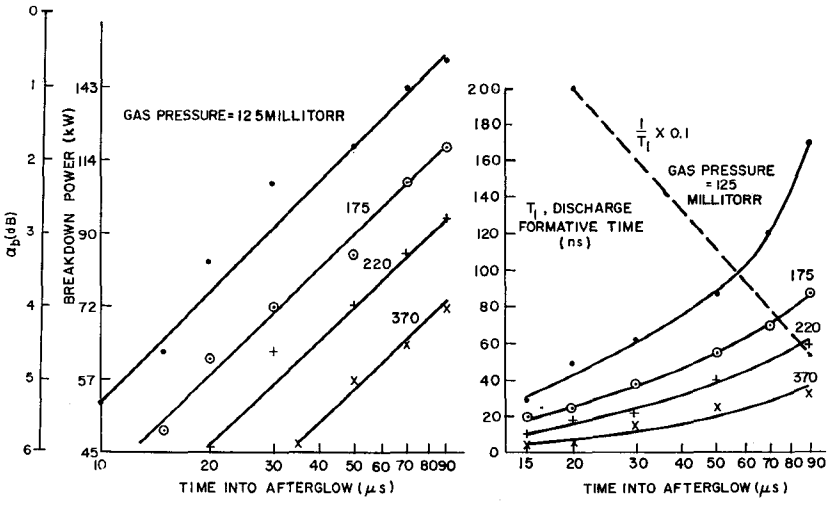

Fig. 12. α_b and T_1 as a function of remanent density with pressure as a parameter.

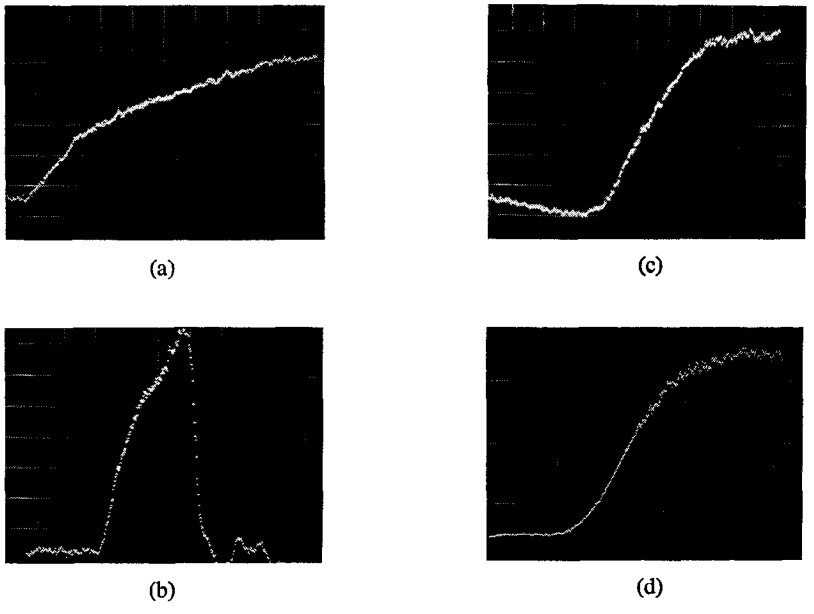

Fig. 13. Operating waveforms viewed on HP 185 sampling oscilloscope. All traces are synchronized from RF source pulse. (a) Source pulse: $y=40$ kW/div, $x=10$ ns/div. (b) Transmitted power: $y=10$ kW/div, $x=5$ ns/div. (c) Power reflected from TWS No. 1: $y=10$ kW/div, $x=1$ ns/div. (d) Power incident on TWS No. 2: $y=10$ kW/div, $x=1$ ns/div.

plot on a log scale as expected from (2). Note that $1/T_1$ is also a linear function at constant pressure on a log plot.

The experiments were carried out using a 180 kW magnetron source. The ramp function of the high-power magnetron source is shown to rise in Fig. 13(a) from zero to 75 kW in 14 ns and thereupon to rise at a slower rate reading 180 kW in 70 ns. On applying this ramp function to TWS No. 1, the discharge breaks down as shown by the transmitted pulse in Fig. 13(b). The fall of the transmitted pulse T_2 is approximately 2 ns. The rise of the reflected pulse to 70 kW in 3 ns is shown in Fig. 13(c). This same pulse is viewed at port 3 where it rises to approximately 65 kW in 4 ns. The rounding off of the steep wavefront in Fig. 13(c) relative to 13(d) may be due to bandwidth limitations of the circulator.

The useful output pulse for seveal different pressures is shown in Figs. 14 through 16 at power levels of 19, 45, and 70 kW. Table II summarizes the important characteristics of the output pulses. The steep skirt character of the 19 kW pulse is plotted in Fig. 17 from experimental data. Note that the pulsewidth doubles when the power level drops to 1 percent of the peak amplitude.

Experiments were not performed at pressures less than 125 mtorr because the TWS did not trigger properly; the upper pressure limit was set at 400 mtorr because the TWS broke into uncontrolled steady conduction. The influence of rate of rise and magnitude of the applied field, geometry, magnetic fields, gas types, and mixtures were not experimentally investigated. However, increasing the waveguide

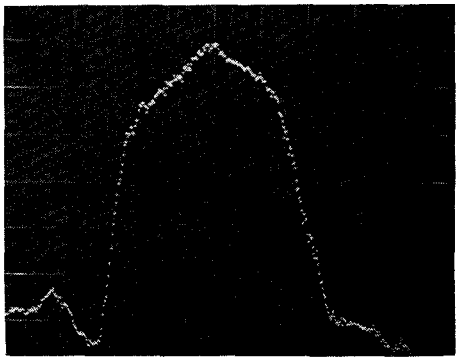

Fig. 14. 10 ns 19 kW X-band output pulse viewed on HP 185 sampling oscilloscope, with delay line. Vertical scale: 3 kW/div; time scale: 2.5 ns/div. The risetime and falltime are 2 and 4 ns, the widths at −10, −13, −20, and −23 dB down from the peak value are 12.5, 15, 20, and 22 ns, respectively.

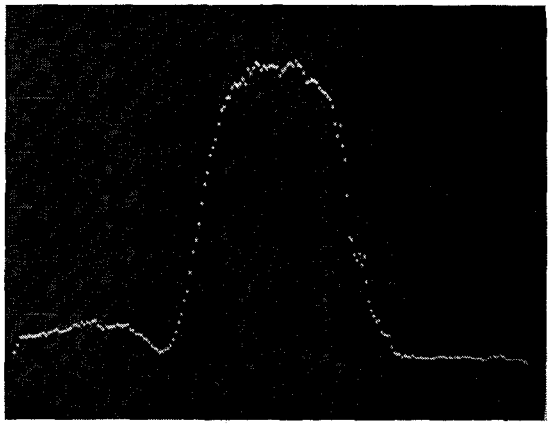

Fig. 15. 6 ns 45 kW X-band output pulse taken with HP 185 sampling oscilloscope with delay line. Synchronized pulse derived from detected envelope of magnetron output pulse before shaping. Time scale: 2 ns/div; risetime: 1 ns; falltime: 2 ns.

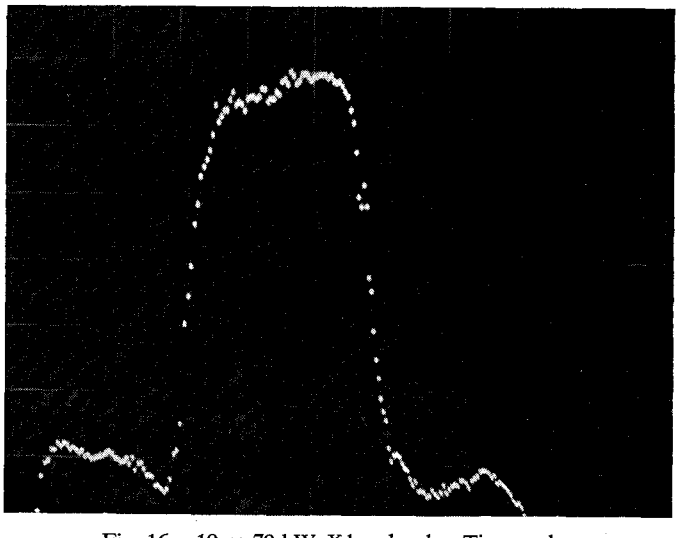

Fig. 16. 10 ns 70 kW X-band pulse. Time scale: 4 ns/div; risetime: 1½ ns; falltime: 2 ns.

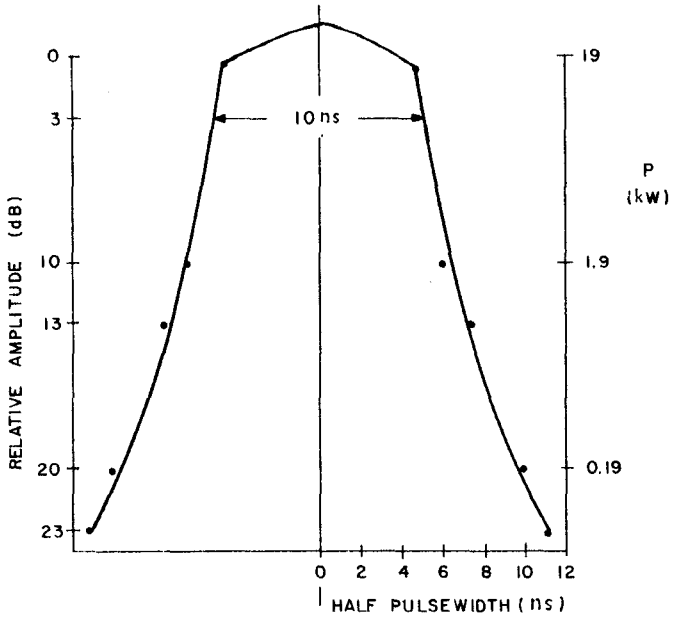

Fig. 17. Skirt characteristics of 19 kW output pulse.

TABLE II

OUTPUT PULSE CHARACTERISTICS

Peak Power (kW)	Risetime (ns)	50% Pulsewidth (ns)	Falltime (ns)	Pulsewidth at −20 dB
19	2	10	3	20
45	1	6	2	11
70	1.5	12	2	24

height for a given power level will decrease the applied field. Placing metallic septums separated by a distance equal to the original height and parallel to the waveguide broadwalls will recover the original geometry-dependent diffusion coefficient. Under equal conditions of n_r and p_0, the power required to break down the gas will rise by the ratio of the waveguide heights. In this way the useful output pulse amplitude may be increased.

APPLICATIONS

Aside from the basic application of the high-power short pulse technique to high-resolution radar systems, there are other uses to which the circuit of Fig. 6 may be applied. By advancing the RF source pulse so that it is incident on TWS No. 1 about 0.2 μs after the exciting beam is initiated, the entire RF pulse is reflected. Operating in this manner effects complete high-power interpulse switching with approximately 60 dB isolation, 0.3 dB arc loss, and 0.2 dB cold loss. By further advancing the RF pulse so that a prescribed fraction of the high-power pulse is transmitted before beam current is initiated, one effects intrapulse switching or pulse splitting.

The above modes of operation, including the short pulse mode, are all derivable from the single circuit of Fig. 6. Operating modes are initiated by selecting the time delay be-

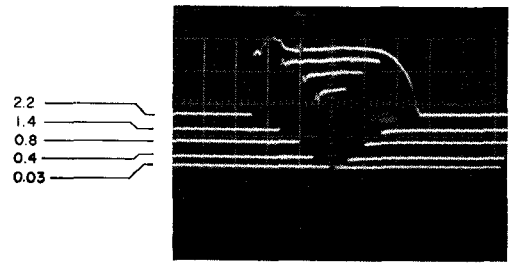

(a)

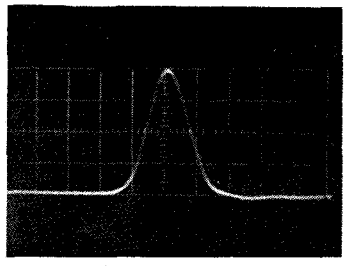

(b)

Fig. 18. Variable pulsewidth operation. (a) Five exposures where $x=0.4$ μs/div. (b) 30 ns pulse where $x=20$ ns/div. Synchronized from magnetron pulse test conditions: $f=9$ GHz, $P=50$ kW, and duty $=0.001$.

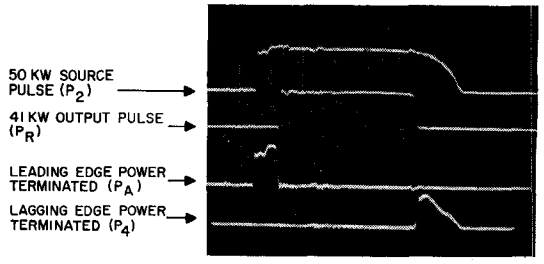

Fig. 19. Pulse shaping at X-band at 50 kW. Radiated pulse characteristics: Rise and falltimes $=14$ ns; half-power pulsewidth $=1.4$ μs increasing to 1.6 μs at -40 dB.

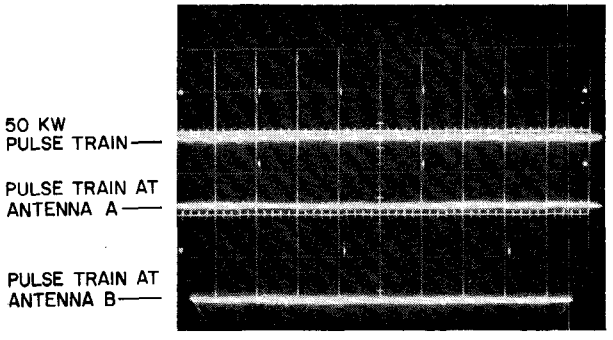

Fig. 20. Antenna sharing of a single source.

tween trigger pulses applied to the TWS, each of which is appropriately delayed relative to the RF source pulse. The video trigger required to actuate the TWS is a 100 volt 0.5 μs pulse from a source whose impedance is 500 ohms.

Operation as an intrapulse switch at 50 kW in X band is shown in Fig. 18. The multiple exposure depicts several pulsewidths all of which are derivable from a single source. A discrete width can be ascribed to each radiated pulse from 30 ns up to 2.2 μs. The switching speed, skirt attenuation rate in decibels per nanoseconds and switching jitter are independent of the pulsewidth modulating rate up to the PRF of the source modulator. An example of intrapulse switching to clean up a magnetron pulse is depicted in Fig. 19. Note the significant improvement in the lagging edge. Interpulse switching to effect time sharing of two or more antennas was experimentally tried at 50 kW, 0.002 duty as shown in Fig. 20. Alternate pulses were directed to two antennas although any fraction of pulses in the train can be fed to either antenna since the high-power switches are controlled by a low-voltage video trigger pulse susceptible to a programmed logic. The operational modes are given in Table III.

TABLE III

OPERATIONAL MODES OF BASIC CIRCUIT

Modes	Classification	Actuating Signal
Short pulse source	intrapulse	RF self breakdown
Variable resolution	intrapulse	video trigger
Antenna sharing	interpulse	video trigger
Pulse shaping	intrapulse	video trigger

CONCLUSIONS

No attempt has been made to experimentally study the effect of geometry, gas type, gas mixtures, and rate of rise of the applied field on the enhancement of the output pulse; therefore, we must conclude that much work directed toward increasing the output–input pulse amplitude ratio still remains to be done. The results obtained in this study do show the feasibility of generating short pulses on a nanosecond scale at kilowatt levels from a combination of ordinary microwave components, i.e., a circulator, a high-power source, and two waveguide sections containing a low-pressure gas.

REFERENCES

[1] A. A. Dougal and L. Goldstein, "The spike in transmit-receive (TR) tubes," *IRE Trans. Electron Devices*, vol. ED-3, pp. 142–148, July 1956.

[2] A. D. MacDonald, "High frequency breakdown in air at high altitudes," *Proc. IRE*, vol. 47, pp. 436–441, March 1959.

[3] A. D. MacDonald, D. V. Gaskell, and H. N. Gitterman, "Microwave breakdown in air, oxygen, and nitrogen," *Phys. Rev.*, vol. 130, no. 5, June 1963.

[4] H. Goldie, "A fast broadband high power microwave switch," *Microwave J.*, August 1963.

[5] L. Gould and L. W. Roberts, "Breakdown of air at microwave frequencies," *J. Appl. Phys.*, vol. 27, no. 10, October 1956.

[6] L. Goldstein, A. A. Dougal, and W. H. Christoffers, "Final report on TR tube spike leakage investigation," Research Lab., University of Illinois, Urbana, October 1955.

[7] S. C. Brown, *Basic Data of Plasma Physics*, 2nd ed. New York: Wiley, 1959.

[8] R. M. Hill and S. K. Ichiki, "Microwave switching with low-pressure arc discharge," *IRE Trans. Microwave Theory and Techniques*, vol. MTT-8, pp. 628–633, November 1960.